Voltammetric Studies of Gold, Protons, and [HCl2]− in Ionic Liquids

ARTICLE *in* THE JOURNAL OF PHYSICAL CHEMISTRY C · JUNE 2007

Impact Factor: 4.77 · DOI: 10.1021/jp0709555

6 AUTHORS, INCLUDING:

Leigh Aldous
University of New South Wales
89 PUBLICATIONS **1,836** CITATIONS
SEE PROFILE

Debbie S. Silvester
Curtin University
55 PUBLICATIONS **1,684** CITATIONS
SEE PROFILE

Voltammetric Studies of Gold, Protons, and $[HCl_2]^-$ in Ionic Liquids

Leigh Aldous,[†] Debbie S. Silvester,[‡] William R. Pitner,[§] Richard G. Compton,[‡] M. Cristina Lagunas,*[,†] and Christopher Hardacre*[,†]

The QUILL Centre/School of Chemistry and Chemical Engineering, Queen's University, Belfast, BT9 5AG, Northern Ireland, United Kingdom, Physical and Theoretical Chemistry Laboratory, University of Oxford, South Parks Road, Oxford OX1 3QZ, United Kingdom, and Merck KGaA, PLS Ionic Liquids, Frankfurter Strasse, 64271 Darmstadt, Germany

Received: February 3, 2007; In Final Form: March 22, 2007

The comparative study of the voltammetry of $H[NTf_2]$, HCl and $H[AuCl_4]$ in $[C_4mim][NTf_2]$ has provided an insight into the influence of protons on the reduction of $[AuCl_4]^-$ at Au, Pt or glassy carbon (GC) electrodes, and has allowed the identification of an unprecedented proton-induced electroless deposition of Au on relatively inert GC surfaces. For the first time, clear evidence of the quantitative formation of $[HCl_2]^-$ has been obtained in $HCl/[C_4mim][NTf_2]$ mixtures, and the electrochemical behavior of these mixtures analyzed. In particular, a significant shift of the dissociation equilibrium toward the formation of chloride and the solvated proton (H_{IL}^+), following electrochemical reduction of H_{IL}^+ has been observed in the time-scale of the experiments.

Introduction

Ionic liquids (ILs) are liquids composed entirely of ions which display negligible vapor pressures and typically possess high ionic conductivities.[1,2] Their inherent conductivity allows electrochemical investigations to be carried out in ILs without additional supporting electrolyte. The ionic nature of ILs allows the stabilization and subsequent electrochemical investigation of certain species which are otherwise difficult to isolate, e.g., PCl_3 and $POCl_3$[3] due to their unique solvating abilities. In addition, their wide electrochemical windows have encouraged investigation into the deposition and redox behavior of a wide range of metals in these solvents.

There are many studies concerning gold in ILs, including the effect of the IL on the surface structure of single-crystal gold electrodes,[4−7] the electrodeposition of gold nanoparticles from $[Au(CN)_2]^-$-based ILs,[8] and the electrodeposition of metals (e.g., Ge, Ni, Co, Cu, Ag, Al, Si, Sn, and Zn) on various Au surfaces.[5,9−11] In many of these systems the formation of alloys were reported. However, only a limited number of electrochemical investigations have been performed on dissolved gold compounds. Xu and Hussey studied dissolved $[AuCl_4]^-$ at a glassy carbon (GC) electrode using a Lewis basic aluminum chloride-1-ethyl-3-methylimidazolium chloride ionic liquid ($AlCl_3$-$[C_2mim]Cl$).[10] Therein, two reduction waves were observed corresponding to the reduction of $[AuCl_4]^-$ to $[AuCl_2]^-$ and Au(0) deposition. Oxidative dissolution of the Au deposit was also observed, generating $[AuCl_2]^-$. Similarly, Sun et al.[12] demonstrated that reduction of Au(I) lead to deposition of metallic gold at a glassy carbon (GC) electrode and subsequent anodic stripping of the deposit to Au(I) in a Lewis basic 1-ethyl-3-methylimidazolium chloride-tetrafluoroborate ionic liquid.

We have recently reported a detailed study of the electrochemistry of $Na[AuCl_4]$ in $[C_4mim][NTf_2]$ at Au, Pt and GC working electrodes, and of pure Au in the presence of chloride.[13] The $Na[AuCl_4]$ was reduced in all cases by two successive reductions, leading to the deposition of gold. Following reduction and deposition of gold, all three electrode materials displayed three oxidation processes on the reverse sweep. Two corresponded to the two-step oxidation of Cl^- at the freshly deposited gold surface[13,14] while the third was attributed to the chloride-initiated dissolution of Au into the IL via the oxidative formation of surface layers of AuCl.

Extensive research has been performed on protons in the haloaluminate IL systems, both due to their persistent appearance as unwanted impurities, and as active reagents.[15] Protons in chloroaluminate ionic liquids are frequently superacidic, with Hammett acidities of up to -18.[15] In basic chloroaluminate ionic liquids (excess chloride) the formation of $[HCl_2]^-$, as well as higher species such as $[H_2Cl_3]^-$ and $[H_3Cl_4]^-$, has previously been demonstrated.[15,16] In non-haloaluminate ILs, the exact nature and relative strength of acidic protons when dissolved in ionic liquid systems is still a topic of intense scrutiny. For example, Friedel−Crafts reactions in ionic liquids based upon the bis{(trifluoromethyl)sulfonyl}imide anion, $[NTf_2]^-$, the acid catalysts $H[BF_4]$ and H[OTf] demonstrate significantly lower reaction rates than $H[NTf_2]$, despite all three being strong acids in water.[17] Conventional acid−base indicators have been used to physically probe the inherent acidity and passivity of ionic liquids; however, such probes are not calibrated for ionic liquids and the observed color changes are the result of a combination of hydrogen-bonding interactions and the acid−base equilibria.[18,19] In an effort to better understand the nature of protons in the IL environment, Del Popolo et al. carried out a first-principles simulation study, simulating the dissolution and solvation of HCl in the ionic liquid $[C_1mim]Cl$.[20] However, rather than dissociation, the rapid formation of the anion $[HCl_2]^-$ was observed. Silvester et al. recently investigated the electrochemical oxidation of dissolved hydrogen gas in a range of ILs, and found that the resulting H^+ species was sufficiently stable to be observed for a range of anions with the exception of chloride.[21]

* Corresponding authors. Tel.: +44 28 9097 4592. Fax: +44 28 9097 4687. E-mails: c.lagunas@qub.ac.uk, c.hardacre@qub.ac.uk.
[†] Queen's University.
[‡] University of Oxford.
[§] Merck KGaA.

10.1021/jp0709555 CCC: $37.00
Published on Web 05/26/2007

TABLE 1: Summary of the Proposed Reactions, Peak Assignments, and Equation Numbers

peak	eq	proposed reactions
I	1	$H_{IL}^+ + e^- \rightarrow H_{ads}$
	2	and $2H_{ads} \rightarrow H_2$
	3	or $H_{ads} + H_{IL}^+ + e^- \rightarrow H_2$
II		$H_2O \rightarrow 1/2H_2 + OH^-$
III		proton mediated anion oxidation
IV		reduction of monolayer formed by III
V	5	$[HCl_2]^- \rightarrow H_{IL}^+ + Cl_2 + 2e^-$
VI	6	$3Cl^- \rightarrow Cl_3^- + 2e^-$
VII	7	$Cl_3^- \rightarrow 3/2Cl_2 + 1e^-$
VIII		$H^+_{IL} + Cl_2 + 2e^- \rightarrow [HCl_2]^-$
IX	8	$Cl_2 + 2e^- \rightarrow 2Cl^-$
X		$2Cl^- \rightarrow Cl_2 + 2e^-$
XI	10	$Au_{surface}Cl^- \rightarrow AuCl_{surface} + e^- \rightarrow$ further oxidative dissolution
XII		reduction of dissolution by-products
XIII		reduction of dissolution by-products
XIV	9	$[AuCl_4]^- + 2e^- \rightarrow [AuCl_2]^- + 2Cl^-$
XV	11	$[AuCl_2]^- + 1e^- \rightarrow Au(0) + 2Cl^-$
		$H_{IL}^+ + e^- \rightarrow \rightarrow H_2$
XVI		reduction and UPD of $H[AuCl_4]$ at active sites on GC

Herein, we describe the electrochemical investigation of $H[NTf_2]$, HCl, and $H[AuCl_4]$ in 1-butyl-3-methylimidazolium bis{(trifluoromethyl)sulfonyl}imide ($[C_4mim][NTf_2]$) carried out at GC, Pt and Au electrodes. The reduction processes of the solvated proton (H_{IL}^+) are discussed in detail as well as the quantitative formation of $[HCl_2]^-$ upon dissolution of HCl, in order to understand the complex electrochemistry of $H[AuCl_4]$. Interestingly, from this study, the unexpected electroless deposition of Au at GC was observed.

Experimental

Chemical Reagents. 1-Butyl-3-methylimidazolium chloride ($[C_4mim]Cl$) and 1-butyl-3-methylimidazolium bis{(trifluoromethyl)-sulfonyl}imide ($[C_4mim][NTf_2]$) were prepared in house using standard literature methods.[1] Hydrogen tetrachloroaurate trihydrate ($H[AuCl_4]\cdot 3H_2O$) (Alfa Aesar) and bis{(trifluoromethyl)-sulfonyl}imide ($H[NTf_2]$, Fluka, >95%) were used as received. Tetraethylammonium dichloroaurate ($[N_{2222}][AuCl_2]$) was prepared as previously described.[13] $[C_4mim][NTf_2]$ was dried for >96 h under high vacuum at 70 °C prior to use, the resulting IL containing a residual water content of <0.01 wt % as determined by Karl Fischer titration. The IL was then stored in a N_2-filled glove box, and all solutions were prepared in the glove box prior to use.

Instrumentation. Voltammetric experiments were carried out in a 10 cm^3 glass cell with 3 g of ionic liquid. Cyclic voltammograms were recorded with a PC controlled Potentiostat/Galvanostat EG&G Model 273A, and performed with a three-electrode arrangement with a glassy carbon (3 mm diameter), platinum (1.6 mm diameter) or gold (1.6 mm diameter) working electrode, a bright platinum mesh as the counter electrode, and all potentials measured with respect to a 0.01 M Ag^+/Ag reference, with $AgNO_3$ dissolved in $[C_4mim][NO_3]$ and separated from the bulk solution via a glass frit. The *IR*-drop was uncompensated. The glassy carbon electrode was polished using diamond pastes (Kemet, U.K.) of decreasing particle size (6 - 0.1 μm) on soft lapping pads. The Au and Pt electrodes were polished with 5 μm, 1 μm and 0.01 μm alumina slurries on lapping pads. All peak assignments for the cyclic voltammograms have been summarized in Table 1. Prior to all experiments, the solutions were removed from the glovebox and purged by bubbling dry argon for at least 10 min. A slight positive pressure of inert gas was maintained above the surface of the electrolyte throughout the experiments to limit contamination.

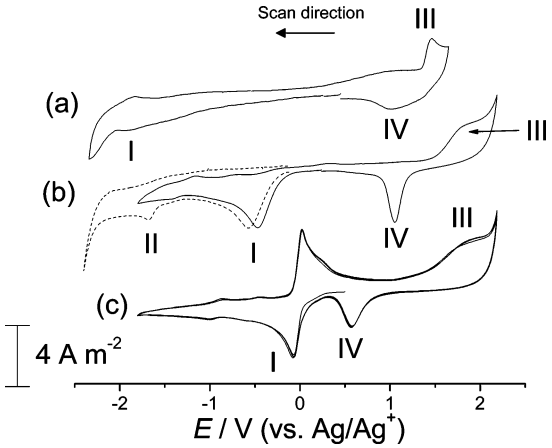

Figure 1. Offset cyclic voltammograms of 15 mM $H[NTf_2]$ dissolved in $[C_4mim][NTf_2]$, at (a) GC, (b) Au, and (c) four cycles at Pt, obtained at a scan rate of 100 mV/s. Also shown in panel (b) is 15 mM $H[NTf_2]$ in $[C_4mim][NTf_2]$ at Au after the addition of 45 mM H_2O (---).

All solutions of anhydrous HCl in $[C_4mim][NTf_2]$ were generated by the introduction of a small amount of anhydrous HCl gas into the dry argon-filled headspace of the cell before stirring the electrolyte for 30 s. Direct bubbling of the gas yielded similar solutions but at impractically high concentrations. The solutions were also shorted lived (ca. 5 min before noticeable decreases in the HCl concentration), and this prevented subsequent analytical determination of the concentrations investigated, as well as generation of known concentrations of HCl via the mixing of $H[NTf_2]$ and $[C_4mim]Cl$.

Glassy carbon pieces (from glassy carbon plate, Alfa Aesar, type 1) were washed with ethanol and air-dried before use. For the electroless deposition experiments, the glassy carbon was immersed in a 15 mM solution of $H[AuCl_4]$ or $Na[AuCl_4]$ in $[C_4mim][NTf_2]$ while in a nitrogen filled glovebox for 7 days. For scanning electron miscrosopy (SEM) examination, the samples were removed and rinsed gently with acetonitrile, before being mounted upon aluminum stubs with silver epoxy. All samples were analyzed using a JEOL 6500 FEGSEM at 5 kV.

Results and Discussion

$H[NTf_2]$ in $[C_4mim][NTf_2]$. The voltammetries of a 15 mM solution of $H[NTf_2]$ in $[C_4mim][NTf_2]$ using GC, Au and Pt electrodes are shown in Figure 1. Over Pt and Au, one sharp reduction process is observed, denoted as peak I. This was found to be electrochemically reversible on Pt whereas on Au no corresponding oxidative waves are observed. In contrast, over GC, a single very broad feature is observed, I. The peak potentials shift progressively more cathodic on changing the electrode from Pt to Au to GC, in agreement with the relative hydrogen overpotential of the electrode materials, i.e., GC $\gg$ Au > Pt.[22]

The reduction of $H[NTf_2]$ has recently been investigated in $[C_2mim][NTf_2]$ and $[C_4mim][NTf_2]$ at a Pt microelectrode by Silvester et al.[21] Therein, two overlapping reduction peaks were frequently observed which were attributed to two competing reduction pathways, with initial H_{IL}^+ adsorption (eq 1) followed by H_2 formation via eqs 2 and/or 3:[21]

$$H_{IL}^+ + e^- \rightarrow H_{ads} \quad (1)$$

$$2H_{ads} \rightarrow H_2 \quad (2)$$

$$H_{ads} + H_{IL}^+ + e^- \rightarrow H_2 \quad (3)$$

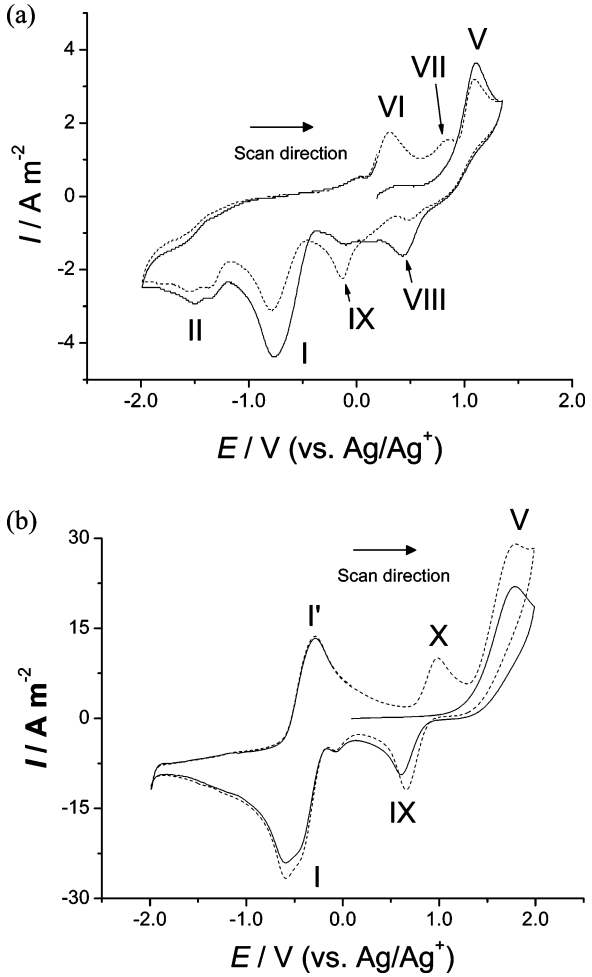

Figure 2. Cyclic voltammograms of HCl gas taken up in $[C_4mim][NTf_2]$, displaying first (—) and second (---) cycles using (a) an Au electrode and (b) a Pt electrode at a scan rate of 100 mV s^{-1}.

In this present work, a small irreversible feature at −1.66 V, peak II, was often observed on the CVs at Au, following initial proton reduction, which typically gave a small, poorly defined anodic peak on the reverse scan. However, it was observed that this grew upon the addition of water (dashed inset in Figure 1), and a scan of 45 mM H_2O in pure $[C_4mim][NTf_2]$ gave a similar peak, confirming that this corresponded to the reduction of water.

On scans at Au and Pt, an oxidation peak, III, is observed which is followed by a reduction peak consistent with desorption of an adsorbed species, IV. Similar features were observed by Silvester et al. at a Pt microelectrode and was assigned to the oxidation of $H[NTf_2]$.[21] The oxidation product of the $[NTf_2]^-$ anion has been postulated by MacFarlene et al.[23] to be the radical $[N\cdot(SO_2CF_3)_2]$, which may form at lower potentials in the presence of protons, i.e., as observed in this case where peak III occurs just prior to the bulk oxidation of $[NTf_2]^-$. The adsorbed species formed have previously been shown to be reduced on the reverse scan to form a monolayer of hydrogen atoms on the electrode surface.[21] Interestingly, similar adsorption and desorption processes are also observed at the nonmetallic GC surface.

HCl in $[C_4mim][NTf_2]$. Figure 2a shows an anodic scan of a HCl/$[C_4mim][NTf_2]$ solution using an Au electrode. It should be noted that the appearance of the voltammogram is a consequence of the low HCl concentration and unexpected resistance in the frit of the reference electrode, which forced the recording of scans at enlarged current windows. On scanning from +0.19 V, no oxidative process (including the anticipated oxidation of Cl^-, covered later) is observed prior to an oxidative peak, V, at +1.09 V. It is thought that the HCl is in the form of hydrogen dichloride, $[HCl_2]^-$, via the equilibrium shown in eq 4, and peak V may be attributed to the two-electron oxidation of $[HCl_2]^-$ forming chlorine, eq 5:

$$H_{IL}^{+} + 2Cl^- \rightleftharpoons [HCl_2]^- \quad (4)$$

$$[HCl_2]^- \rightarrow H_{IL}^{+} + Cl_2 + 2e^- \quad (5)$$

The fact that a separate oxidation peak is observed suggests that $[HCl_2]^-$ is formed as a stable, discrete species in the IL, which is not unexpected. This species has been identified in ionic liquids following the addition of HCl gas to $[C_2mim]Cl$ forming $[C_2mim][HCl_2]$[24,25] as well as in basic haloaluminate melts.[16,26] However, this is believed to be the first observation of $[HCl_2]^-$ in an $[NTf_2]^-$-based IL, and the first electrochemical investigation of this species in a non-haloaluminate IL. On the reductive sweep, the reduction of the solvated proton (H_{IL}^+), peak I, is observed at −0.74 V, as shown for $H[NTf_2]$ in $[C_4mim][NTf_2]$ in Figure 1. Peak II was also observed at −1.48 V, implying minor water contamination. Interestingly, on the return oxidative sweep two new peaks are observed, VI and VII, which were absent on the initial cycle. Peaks VI and VII have previously been assigned to the oxidation of chloride to trichloride and trichloride to chlorine, via eqs 6 and 7, respectively.[3,13,14] The apparent generation of Cl^- (as opposed to $[HCl_2]^-$) may be associated with the removal of the solvated protons during the reductive sweep, causing the eq 4 to shift in favor of the free chloride, which can in turn be observed on the time scale of the experiment due to slow diffusion in the ionic liquid system:[27]

$$3Cl^- \rightarrow Cl_3^- + 2e^- \quad (6)$$

$$Cl_3^- \rightarrow \frac{3}{2}Cl_2 + e^- \quad (7)$$

Two further peaks are observed on the reduction cycle at +0.43 V (peak VIII) and −0.13 V (peak IX), which are present on both the first and second sweeps. These are believed to be related to the reduction of Cl_2 following oxidation of $[HCl_2]^-$, eq 5, or Cl^-, eqs 6−7. However, only peak IX corresponds well to the previously reported reduction of Cl_2 via eq 8, reported at −0.15 V versus Ag/Ag^+ for 15 mM Cl^- (from $[C_4mim]Cl$) in $[C_4mim][NTf_2]$ over an Au electrode.[13] The disparity in the case of peak VIII is attributed to the local high concentration of protons as a result of the oxidation of $[HCl_2]^-$ which could facilitate the reduction of Cl_2 via the reverse reaction of eq 5. This is expected to result in the formation $[HCl_2]^-$ and lead to the observed anodic shift, relative to reduction leading to Cl^-. Some changes in the relative size of peaks VIII and IX are observed between the first and second sweep. However, the total area of VIII + IX remains equal and therefore the changes are believed to be related to the previously noted changes in the local concentration of solvated protons:

$$Cl_2 + 2e^- \rightarrow 2Cl^- \quad (8)$$

The formation of $[HCl_2]^-$ from HCl would also be expected to yield a solvated proton. In this case the observation of the adsorption peak III (Figure 1b) and corresponding desorption peak, IV, should be observed after carrying the scan beyond

peak V (e.g., >+1.35 V). However, this could not be confirmed as in all cases this area was dominated by the chloride-induced gold stripping peak XI. These processes are discussed in more detail below.

Plots of the limiting current versus the square root of the scan rate gave linear plots for all peaks in Figure 2a, implying all processes are diffusion controlled.

Similar observations were found for HCl in $[C_4mim][NTf_2]$ over a Pt electrode (Figure 2b). On the first anodic scan, oxidation of $[HCl_2]^-$ was observed at $E_{1/2}$ of +1.79 V, V, which generated a reduction peak corresponding to the reduction of Cl_2 at +0.58 V, IX.[13] Continuing the reverse scan revealed well-defined proton reduction and oxidation peaks at −0.58 V, I. It is noted here that for HCl solutions, proton reduction I occurs ca. 0.50 V more cathodically than $H[NTf_2]$ solutions. This is likely due to the differing acidity of the two protons as discussed below. On the return anodic scan, a second oxidative process, peak X, was observed in addition to peak V. Peak X corresponds to the previously reported oxidation of free Cl^- at +0.98 V via the reverse reaction shown in eq 8.[13]

A small prepeak to I was also observed at −0.1 V as well as a broadening of peak I. The two competing mechanisms reported by Silvester et al.[21] and shown by eqs 2 and 3 are thought to account for the broadening of peak I observed in Figure 2b. However, the prepeak has not been reported and was not present in the pure IL, and may be associated with reduction of the proton at a range of sites on the polycrystalline Pt electrode surface.

In contrast to Pt and Au electrodes, for HCl dissolved in $[C_4mim][NTf_2]$ GC showed a featureless oxidative window prior to the breakdown of the solvent (not shown). However, if a cathodic scan was carried beyond the onset of the solvated proton reduction, shown by a broad peak similar to peak I observed for $H[NTf_2]$, the reverse scan revealed both an oxidative peak associated with the oxidation of Cl^- (e.g., X), as well as the corresponding Cl_2 reduction peak (IX). These peaks were observed to grow as the cathodic limit of the initial scan was increased, i.e., as more protons are reduced. On the anodic scans, no processes were observed prior to the expected exponential increase in current at the limit of the oxidative electrochemical window (>+1.75 V). This shows that, at GC, $[HCl_2]^-$ has an oxidation potential which is at least as high as $[NTf_2]^-$.

These observations indicate that when HCl dissolves in $[C_4mim][NTf_2]$ the equilibrium shown in eq 4 is formed. The position of the equilibrium between solvated proton and Cl^- or $[HCl_2]^-$ can be altered on the time scale of the experiment by the reduction of protons at either Au, Pt or GC electrodes. Silvester et al. have previously demonstrated that solvated protons, generated by the reduction of H_2 at a Pt electrode, are sufficiently stable on the time scale of the experiment to generate a reversible wave in a number of ILs, including $[C_4mim][NTf_2]$.[21] Once dissolved the proton is believed to form an as-yet undetermined solvated species, for example $(H_x[NTf_2]_y)^{x-y}$. Silvester et al. also observed a completely irreversible solvated proton reduction wave in $[C_6mim]Cl$,[21] which was believed to correspond to the rapid loss of H^+ as $[HCl_2]^-$ and is in good agreement with the present work.

The diffusion coefficient of the $[HCl_2]^-$ was not determined in this study due to the short-lived nature of the solutions and the difficulty in measuring the concentration of HCl. Significant desorption of HCl from the ionic liquid was observed after 5 min following the introduction of the gaseous HCl, and a blank electrochemical window could be obtained after brief bubbling of Ar through the solution. Similar problems have also been reported for the study of protons in haloaluminate ILs.[28,29] This work demonstrates that only through the use of sealed cells or variable pressure cells, such as that previously described by Campbell and Johnson,[26] can precise mixtures of HCl in $[NTf_2]$-based ILs be quantitatively investigated.

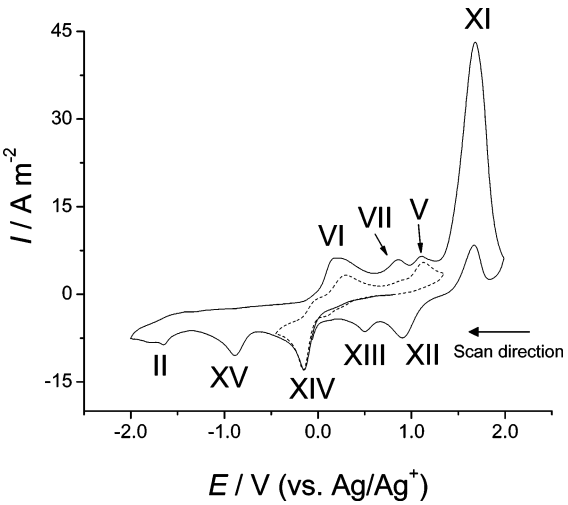

Figure 3. Cyclic voltammograms of 15 mM of $H[AuCl_4]$ dissolved in $[C_4mim][NTf_2]$, displaying a complete (—) and restricted cycle (---) using an Au electrode and a scan rate of 100 mV s^{-1}.

$H[AuCl_4]$ in $[C_4mim][NTf_2]$ at Au, Pt and GC Electrodes. Figures 3 and 4 show the cyclic voltammograms for a 15 mM solution of $H[AuCl_4]$ in $[C_4mim][NTf_2]$ at Au and Pt electrodes, respectively. The voltammetry over both electrodes show a number of similar features to those previously reported for $Na[AuCl_4]$ in $[C_4mim][NTf_2]$,[13] namely the two-electron reduction of $[AuCl_4]^-$ to $[AuCl_2]^-$ (peak XIV, eq 9), the two-step oxidation of chloride to chlorine (peaks VI and VII and eqs 6 and 7, respectively), and the oxidative dissolution of gold (peak XI, eq 10). However, a number of additional peaks are also observed for $H[AuCl_4]$, as well as a significant shift/change in shape of the gold deposition feature (peak XV) from the reduction of $[AuCl_2]^-$ (eq 11):

$$[AuCl_4]^- + 2e^- \rightarrow [AuCl_2]^- + 2Cl^- \quad (9)$$

$$Au_{(surface)}Cl^-_{(ads)} \rightarrow AuCl_{(surface)} + e^- \rightarrow \text{further oxidative dissolution} \quad (10)$$

$$[AuCl_2]^- + e^- \rightarrow Au(0) + 2Cl^- \quad (11)$$

For $Na[AuCl_4]$ in $[C_4mim][NTf_2]$, the reduction of Au(III) to Au(0) resulted in two peaks with peak areas consistent with the expected 2:1 electron ratio.[13] However, for $H[AuCl_4]$, the ratio between the areas of the two reduction peaks, XIV:XV, consistently gave values close to 1:1 (on Au) suggesting that XV is not due solely to the one-electron reduction of $[AuCl_2]^-$ to Au(0). It should be noted that although an enhancement of peak XIII is also clearly observed at Pt and GC electrodes, the ratio XII:XIII could not be precisely determined as the peaks are either not well separated (Pt) or overlap with other processes (GC) (see Figures 4 and 5, respectively).

From the voltammetry of $H[NTf_2]$ on Au, it is proposed that the feature at −0.89 V, denoted as peak XV in Figure 3, is likely to be a combination of deposition of Au as well as the proton reduction (eq 1). A comparison of the position of peak I for $H[NTf_2]$ and peak XV for $H[AuCl_4]$ shows a shift to more negative potentials from −0.65 V to −0.89 V, respectively. The

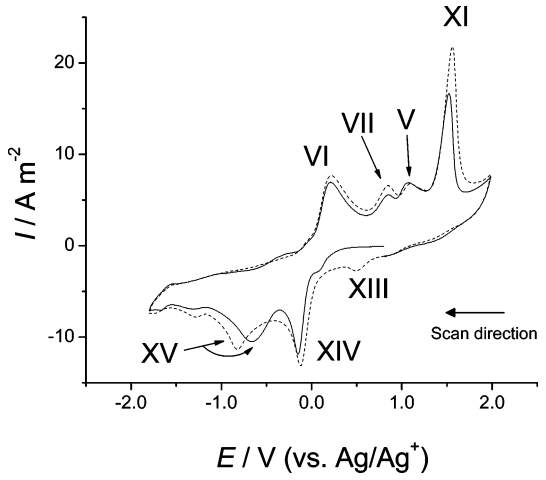

Figure 4. Cyclic voltammograms of 15 mM of H[$AuCl_4$] dissolved in [C_4mim][NTf_2], displaying first (—) and second (---) cycles using a Pt electrode and a scan rate of 100 mV s^{-1}.

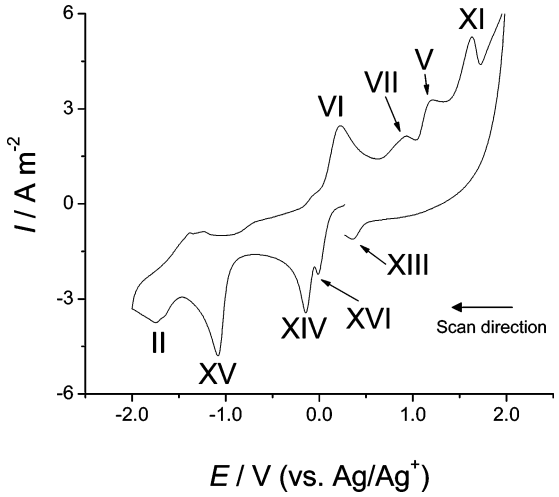

Figure 5. Cyclic voltammogram of 15 mM of H[$AuCl_4$] dissolved in [C_4mim][NTf_2], displaying a complete cycle using a GC electrode and a scan rate of 100 mV s^{-1}.

shift observed for peak I is thought to be related to the presence of Cl^- (from the reduction of $[AuCl_4]^-$, XIV) generating an equilibrium between Cl^- and $[HCl_2]^-$, as suggested by the voltammetry of HCl in [C_4mim][NTf_2]. Since $[HCl_2]^-$ is expected to be less acidic than H[NTf_2], this could account for the shifting of the reduction potential of the solvated proton to higher potentials. Peak II was observed at −1.65 V, which is in good agreement with that found for water in H[NTf_2] solutions, and thus corresponds to the water introduced by the trihydrate H[$AuCl_4$] species used.

Concurrence of peak I and gold deposition has previously been observed in haloaluminate ionic liquids. Xu and Hussey reported an enlargement of the Au(I) to Au(0) reduction peak for $[AuCl_4]^-$ dissolved in a basic [C_2mim]Cl−$AlCl_3$ melt at a GC electrode, and related the change to the presence of protonic-impurities, namely $[HCl_2]^-$.[10] In this case, although the reduction of $[HCl_2]^-$ requires significant overpotential at GC, its reduction at gold was believed to proceed at the same potential required for gold reduction, leading to one peak with enhanced current.[10]

On the return sweep over a gold electrode, four oxidation processes were observed, i.e., peaks VI, VII, V, and XI. Peak V, which was not observed in the case of Na[$AuCl_4$], is associated with the oxidation peak of $[HCl_2]^-$, eq 5, as shown from the study of HCl. The ratio of $[HCl_2]^-$ and Cl^- can be varied by changing the cathodic limit used. Figure 3 clearly shows that if the scan is restricted to −0.5 V, on the subsequent anodic sweep peak V is larger relative to peak VI; i.e., the proportion of $[HCl_2]^-$ has increased over Cl^-. This is consistent with the peak assignments, e.g., following peak XIV, two chloride anions are released into solution for every proton favoring the formation of $[HCl_2]^-$, while following the complete reduction of H[$AuCl_4$] (peak XV), four chloride anions per proton are formed, leading to a mixture with a significant concentration of chloride anions.

In the voltammetry of H[$AuCl_4$] on Pt (Figure 4), the two-electron reduction process, peak XIV, is observed at −0.15 V, with a second reduction wave appearing at −0.66 V, peak XV. Reversing the scan prior to gold deposition (peak XV) showed the appearance of three peaks associated with the formation of Cl_3^-, oxidation of $[HCl_2]^-$ and gold stripping, all of which are consistent with gold-like behavior of the platinum electrode. This may be explained by the fact that some Au is initially deposited on the Pt electrode surface possibly via underpotential deposition (UPD). UPD has been shown by Endres and Freyland for Ge, Ag, Cu and Al on Au(111) in ILs;[11] however, this is not generally found and Xu and Hussey noted that UPD of metals is not common in molten salts compared with aqueous media.[9] As found over Au, peak XV likely corresponds to the concurrent reduction of $[AuCl_2]^-$ and protons. Interestingly, peak XV is found to shift to −0.82 V on the second cycle (cf. peak XV on Au was observed at −0.89 V). This shift may be explained by the fact that the solvated proton is adsorbed and reduced at lower potentials on Pt than Au (cf. Figure 1). This appears to result in the shifting of both the proton reduction and gold deposition processes to more positive potentials on the Pt electrode, and the peak shifts to a more cathodic potential on the second cycle as the electrode gains increasing Au-like behavior.

During the oxidative sweep over platinum, oxidative dissolution of gold, peak XI, was also observed. A comparison of peak XI over gold and platinum electrodes shows that, at the former, the gold oxidation peak is larger and has a hysteresis loop. This trend was also previously observed for Na[$AuCl_4$], and attributed to chloride-induced dissolution of Au continuing beyond the deposited Au layer and into the Au electrode.[13]

Figure 5 displays an anodic scan of 15 mM solution of H[$AuCl_4$] in [C_4mim][NTf_2] at a GC electrode. This is analogous to the voltammetry at Au and Pt electrodes with the features appearing at XIV (−0.15 V), XV (−1.08 V), VI (+0.23 V), VII (+0.93 V), V (+1.21 V), XI (+1.63 V), II (ca. −1.75 V), and XIII (+0.35 V). Peaks XIV and XV correspond to Au reduction at the GC surface while the other peaks are a result of Au-like behavior, as previously seen for Pt. Peak XV is again a combination of Au deposition and proton reduction at the resulting metal surface, and deposition is observed at more anodic potentials relative to Au and Pt by 190 and 420 mV, respectively. This is expected since GC is nonmetallic and, therefore, a less favorable substrate for nucleation and growth.

Furthermore, a prepeak, XVI, to peak XIV was observed at 0.0 V. This prepeak was only observed at a clean GC surface in dry solutions of H[$AuCl_4$], which was also the only system to display an unstable open circuit potential as discussed below.

For all three electrodes, new peaks, XII and/or XIII were observed on the second cycle following Au dissolution at peak XI. Peak XII was observed at +0.90 V on Au and peak XIII was found at +0.49 V on Au and Pt and at +0.35 V for GC. Similar features have also been observed at Au for solutions of Na[$AuCl_4$].[13] These peaks may be related to the reduction of

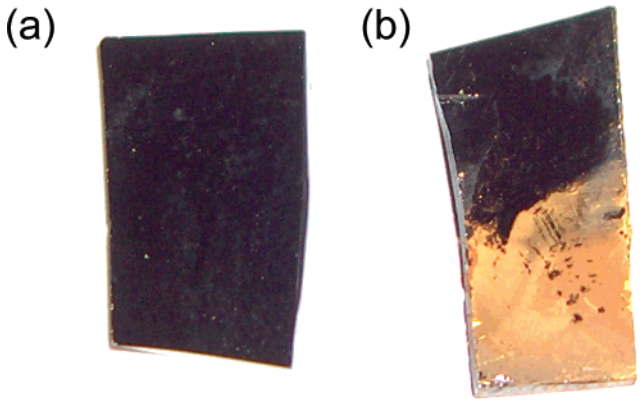

Figure 6. Photograph of (a) clean GC and (b) GC after being held at its OCP for 18 h in a 50 mM solution of $H[AuCl_4]$ in $[C_4mim][NTf_2]$.

complex ions formed as Au dissolution intermediates via the initial formation of AuCl, followed by dissolution and further oxidation, assumed to form short-lived $[AuCl(NTf_2)_x]^{x-}$ species which ligand exchange with free chloride regenerating $[AuCl_4]^-$.[13] It is clear that the peaks are larger at the Au electrode compared with either Pt or GC. This simply reflects the larger reservoir of gold available to form the $[AuCl(NTf_2)_x]^{x-}$ species in the Au macrorelectrode compared to small surface-deposited gold found on the Pt and GC. The lower potential found on GC is consistent with the more difficult gold deposition (and hence more difficult reduction) associated with the nonmetallic substrate.

Equation 4 is written as an equilibrium reaction and in order to test the influence of the equilibrium, 20 mM $[C_4mim]Cl$ was added to a 10 mM solution of $H[AuCl_4]$ in $[C_4mim][NTf_2]$. This resulted in the decrease (XV) or loss (V and XVI) of all peaks associated with protons and generated cyclic voltamogramms similar to that observed for $Na[AuCl_4]$ in $[C_4mim][NTf_2]$.[13] In this case, the addition of chloride leads to the formation of $[HCl_2]^-$ at the expense of the solvated proton and alters the $[AuCl_4]^-$ electrochemical behavior accordingly.

Electroless Deposition of Au. It was observed that upon immersing a GC electrode for 60 min in a solution of 15 mM $H[AuCl_4]$ in $[C_4mim][NTf_2]$, the open circuit potential (OCP) was observed to increase from +0.2 V to a limiting value of +0.8 V. This final OCP was also observed for GC electrodes following the electrochemical deposition of gold. This behavior is in contrast to that observed for $Na[AuCl_4]$ in $[C_4mim][NTf_2]$, where a stable OCP was found for GC, Au and Pt electrodes.[13] On increasing the immersion time to 24 h, clearly visible, isolated gold deposits were observed. Upon increasing the $H[AuCl_4]$ concentration to 50 mM, a gold film was formed after 18 h which covered the GC (Figure 6). The same responses were observed if the solution was kept in the dark, thus discounting the photochemical reduction of gold at the GC surface. If the GC was not connected to the potentiostat, 7 days were required before the formation of visible deposits. This is not due to decomposition of the $H[AuCl_4]$ solution in the $[C_4mim][NTf_2]$ which were otherwise stable for at least 6 months. Interestingly, although no deposition was observed using GC immersed in solutions of $Na[AuCl_4]$ in $[C_4mim][NTf_2]$ even after 14 days, gold deposition was observed after 3 days following the addition of two equivalents of $H[NTf_2]$. The deposition was not found to be affected by the supplier of GC, electrode preparation method or IL cation used, but changing the anion from $[NTf_2]^-$ to $[PF_6]^-$ or $[BF_4]^-$ prevented the gold from nucleating. Interestingly, the presence of water also prevented gold deposits from forming. Using

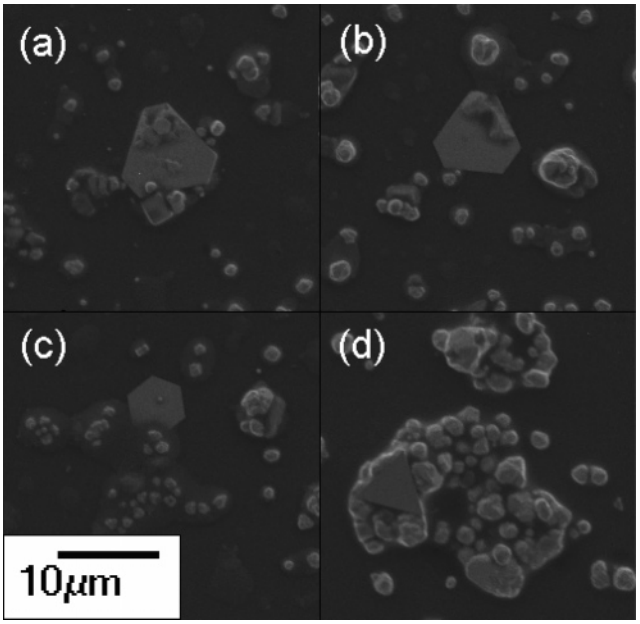

Figure 7. SEM images of gold at a GC substrate under electroless conditions from a 10 mM solution of $H[AuCl_4]$ dissolved in $[C_4mim][NTf_2]$, grown over 7 days under quiescent conditions.

$[C_4mim][NTf_2]$ with a water content >0.01 wt % resulted in the stabilization of the OCP as well as loss of peaks XVI and V with corresponding growth in peaks XIV and VII, until it was similar to the typical voltammogram of $Na[AuCl_4]$. However, the original voltammogram (as observed in Figure 5) could be restored by drying the $H[AuCl_4]$ solution under high vacuum at 40 °C for 24 h.

MacFarlane et al. recently demonstrated that in $[C_4mPyrr][NTf_2]$ the $[NTf_2]^-$ anion is susceptible not only to electrochemical oxidation but also reduction.[23] However, in the present case, Au deposition was observed to begin at an OCP of +0.2 V, which is more than 2 V positive than the reported start of $[NTf_2]^-$ reduction, and more than 1 V negative of the observed oxidation of $H[NTf_2]$ (cf. peak III). It is therefore not likely that the reduction of Au(III) is related to any electrochemical instability of $[NTf_2]^-$. This is further supported by the observation that the addition of water facilitates $[NTf_2]^-$ oxidation[27] and reduction[23] but herein it inhibits the formation of gold deposits.

SEM analysis of GC following immersion in solutions of $H[AuCl_4]$ in $[C_4mim][NTf_2]$ is shown in Figure 7. The surface was found to be covered with irregular, multifaceted growths as well as triangular and 'hexagonal' plates of between 0.1 and 10 μm in size. It is not known whether these shapes formed in solution before precipitating onto the GC or whether they grew from sites on the GC surface. EDAX from the irregular deposits indicated that only gold was present, whereas for the plates, chlorine signals were also observed. These likely correspond to background signals from the substrate below, EDAX of the substrate detecting chloride in addition to the expected signals of GC.

This 'electroless' deposition of gold on the GC surface is likely to be due to reductive sorption of the gold at active sites on the carbon surface. Similar behavior has also been reported for the adsorption and reduction of $H[AuCl_4]$ from aqueous solution using graphitised carbon black, with the graphitic basal planes thought to be the initial adsorption sites prior to the reduction.[30] Reductive sorption of $[AuCl_4]^-$ from hydrochloric acid solutions has also been observed at both activated and

oxidized carbon surfaces.[31] Therein, the activated carbon surfaces containing basic oxygen-based functional groups displayed reductive sorption of $[AuCl_4]^-$ via electrochemical mechanisms, while acidic oxygen-based functional groups displayed chemical reduction mechanisms.[31] Suzer and Dag have also reported that $[AuCl_4]^-$ can undergo reductive deposition to Au(0) from aqueous solution at any surface which can provide an active adsorption site.[32] Therefore, in the present case, it is probable that the reductive sorption of $[AuCl_4]^-$ occurs at surface defects or impurities in the GC electrode, with protons either activating these sites or otherwise facilitating the reduction process of $[AuCl_4]^-$ in the IL. For example, it is possible that adsorption results in the reduction of $[AuCl_4]^-$ to $[AuCl_2]^-$, and the presence of H^+ then encourages the deposition of gold, potentially via the disproportionation of $[AuCl_2]^-$. This is supported by the observation that the addition of small quantities of $H[NTf_2]$ to $[N_{2222}][AuCl_2]$ in $[C_4mim][NTf_2]$ resulted in the immediate, apparent reduction of $[AuCl_2]^-$ to yield an opaque golden suspension, from which gold particles settled as a fine powder within 48 h. Identification of the active functional groups might facilitate the electroless recovery of gold from IL solutions, as well as offering a method for gold patterning and modifying otherwise inert substrates, e.g., glassy carbon, via prior surface treatment.

Given that similar deposition has been observed from aqueous solutions, it is unlikely that the decrease in deposited gold in the presence of water is associated with water adsorbing and deactivating the GC sites, and more likely corresponds to water altering the chemical activity or pK_a of the solvated proton within the IL. This effect could also be explained by complexation or hydrolysis[33] of the Au(III) species which might reduce the affinity of the gold species for the surface.

The prepeak XVI was only observed for CVs of $[AuCl_4]^-$ in the presence of H^+ on the first cycle on a polished GC electrode, and could only be regenerated following abrasive cleaning of the electrode surface, either by wiping with an acetonitrile-soaked tissue or polishing. Leaving the GC electrode immersed at its OCP for several minutes before initiating the scan resulted in a decrease in the definition of XVI, which merged into peak XIV. Given that XVI was only observed at GC electrodes where 'electroless' gold deposition was found, peak XVI is thought to be due to the 'underpotential deposition' and nucleation of gold at active sites on the GC surface.

Conclusions

The reduction of $H[NTf_2]$ in $[C_4mim][NTf_2]$ was investigated at Pt, Au and GC electrodes. Two features associated with H_2 formation were observed. These have been tentatively attributed to the reduction of the solvated proton and reduction of an adsorbed species formed via proton mediated oxidation of $[NTf_2]^-$. Interestingly, HCl gas dissolves in $[C_4mim][NTf_2]$ to form $[HCl_2]^-$, which is in equilibrium with H_{IL}^+ and Cl^- as demonstrated by the voltammetry of $HCl/[C_4mim][NTf_2]$ mixtures. Initial anodic scans are clearly dominated by the two-electron oxidation of $[HCl_2]^-$, showing that this is the main species present in solution. However, the extent of the equilibrium can be altered. By cycling through the solvated proton reduction peaks in the cathodic sweep, and effectively removing the solvated proton from the mixture, the features associated to Cl^- are observed to appear in the reverse scan.

These detailed studies on the voltammetry of $H[NTf_2]$ and HCl, together with previous work on $Na[AuCl_4]$, have allowed a good understanding of the complex voltammetry of $H[AuCl_4]$ in $[C_4mim][NTf_2]$. The two-electron reduction from $[AuCl_4]^-$ to $[AuCl_2]^-$ is followed by a combined Au deposition/proton reduction process. Features clearly related to the formation of $[HCl_2]^-$ appear upon release of Cl^- at the Au(III)/Au(I) reduction, and are more evident after the complete reduction to Au(0) and further release of Cl^-. Bulk deposition of Au on Pt was observed to occur at more positive potentials than the deposition of Au on Au. This is believed to result from the combined nature of the solvated proton reduction and Au deposition, proton reduction occurring at more positive potentials on Pt than Au. Surprisingly, the presence of acid also induces the electroless deposition of Au on GC surfaces giving rise to both irregular and highly regular growths. Although the deposition mechanism is still unclear, protons may activate adsorption sites at the GC and/or favor the reduction of Au(III). Interestingly, the deposition is prevented by the addition of water or by changing the anion from $[NTf_2]^-$ to $[PF_6]^-$ or $[BF_4]^-$.

Acknowledgment. L.A. acknowledges support from the Department of Education and Learning in Northern Ireland and Merck KGaA. D.S.S. thanks Schlumberger Cambridge Research for funding via a project studentship.

References and Notes

(1) Bonhôte, P.; Dias, A. P.; Papageorgiou, N.; Kalyanasundram, K.; Grätzel, M. *Inorg. Chem.* **1996**, *35*, 1168.
(2) Silvester, D. S.; Compton, R. G. Z. *Phys. Chem.* **2006**, *220*, 1247.
(3) Silvester, D. S.; Aldous, L.; Lagunas, M. C.; Hardacre, C.; Compton, R. G. *J. Phys. Chem. B* **2006**, *110*, 22035.
(4) Lin, L. G.; Wang, Y.; Yan, J. W.; Yuan, Y. Z.; Xiang, J.; Mao, B. W. *Electrochem. Commun.* **2003**, *5*, 995.
(5) Borisenko, N.; Zein El Abedin, S.; Endres, F. *J. Phys. Chem. B* **2006**, *110*, 6250.
(6) Kubo, K.; Hirai, N.; Tanaka, T.; Hara, S. *Surf. Sci.* **2003**, *546*, L785.
(7) Hirai, N.; Yokogawa, T.; Tanaka, T. *Jpn. J. Appl. Phys.* **2006**, *45*, 2295.
(8) Dobbs, W.; Suisse, J.-M.; Douce, L.; Welter, R. *Angew. Chem., Int. Ed.* **2006**, *45*, 4179.
(9) Xu, X.-H.; Hussey, C. L. *J. Electrochem. Soc.* **1992**, *139*, 1295.
(10) Xu, X.-H.; Hussey, C. L. *J. Electrochem. Soc.* **1992**, *139*, 3103.
(11) (a) Huang, J.-F.; Sun, I.-W. *Adv. Funct. Mater* **2005**, *15*, 989. (b) Zein El Adedin, S.; Endres, F. *ChemPhysChem.* **2006**, *7*, 58. (c) Endres, F.; Schweizer, A. *Phys. Chem. Chem. Phys.* **2000**, *2*, 5455. (d) Endres, F. *Electrochem. Solid-State Lett.* **2002**, *5*, C38. (e) Freyland, W.; Zell, C. A.; Zein El Adedin, S.; Endres, F. *Electrochim. Acta.* **2003**, *48*, 3053. (f) Zell, C. A.; Endres F.; Freyland, W. *Phys. Chem. Chem. Phys.* **1999**, *1*, 697. (g) Zein El Abedin, S.; Moustafa, E. M.; Hempelmann, R.; Natter H.; Endres, F. *Electrochem. Commun.* **2005**, *7*, 1111. (h) Endres, F.; Schrodt, C. *Phys. Chem. Chem. Phys.* **2000**, *2*, 5517. (i) Endres, F. *Phys. Chem. Chem. Phys.* **2001**, *3*, 3165. (j) Endres, F.; Zein El Adedin, S. *Phys. Chem. Chem. Phys.* **2002**, *4*, 1640. (k) Endres, F.; Zein El Adedin, S. *Phys. Chem. Chem. Phys.* **2002**, *4*, 1649. (l) Endres, F.; Zein El Adedin, S. *Chem. Commun.* **2002**, 892. (m) Pitner, W. R.; Hussey, C. L. *J. Electrochem. Soc.* **1997**, *144*, 3095.
(12) Su, F. Y.; Huang, J. F.; Sun, I. W. *J. Electrochem. Soc.* **2004**, *151*, C811.
(13) Aldous, L.; Silvester, D. S.; Villagran, C.; Pitner, W. R.; Compton, R. G.; Lagunas, M. C.; Hardacre, C. *New J. Chem.* **2006**, *30*, 1576.
(14) Villagran, C.; Banks, C. E.; Hardacre, C.; Compton, R. G. *Anal. Chem.* **2004**, *76*.
(15) Welton, T. *Chem. Rev.* **1999**, *99*, 2071.
(16) (a) Trulove, P. C.; Osteryoung, R. A. *Inorg. Chem.* **1992**, *31*, 3980. (b) Campbell, J. L. E.; Johnson, K. E. *J. Electrochem. Soc.* **1994**, *141*, L19. (c) Campbell, J. L. E.; Johnson, K. E. *Inorg. Chem.* **1993**, *32*, 3809.
(17) Hardacre, C.; Katdare, S. P.; Milroy, D.; Nancarrow, P.; Rooney, D. W.; Thompson, J. M. *J. Catal.* **2004**, *227*, 44.
(18) MacFarlane, D. R.; Forsyth, S. A. *A.C.S. Symp. Ser.* **2003**, *856*, 264.
(19) Thornazeau, C.; Olivier-Bourbigou, H.; Magna, L.; Luts, S.; Gilbert, B. *J. Am. Chem. Soc.* **2003**, *125*, 5264.
(20) Del Popolo, M. G.; Kohanoff, J.; Lynden-Bell, R. M. *J. Phys. Chem. B* **2006**, *110*, 8798.
(21) Silvester, D. S.; Aldous, L.; Hardacre, C.; Compton, R. G. *J. Phys. Chem. B.* **2007**, *111*, 5000.

(22) Bockris, J. O'M.; Reddy, A. K. N. In *Modern Electrochemistry 2*; Plenum Press: New York, 1970.

(23) Howlett, P. C.; Izgorodina, E. I.; Forsyth, M.; MacFarlane, D. R. Z. *Phys. Chem.* **2006**, *220*, 1483.

(24) Dyson, P. J.; Grossel, M. C.; Srinivasan, N.; Vine, T.; Welton, T.; Williams, D. J.; White, A. J. P.; Zigras, T. *J. Chem. Soc., Dalton Trans.* **1997**, 3465.

(25) (a) Zawodzinski, T. A., Jr.; Osteryoung R. A. *Inorg. Chem.* **1988**, *27*, 4383. (b) Trulove, P. C.; Osteryoung, R. A.; Sukumaran, D. K. *Inorg. Chem.* **1993**, *32*, 4396. (c) Campbell, J. L. E; Johnson, K. E.; Torkelsont, J. R. *Inorg. Chem.* **1994**, *33*, 3340.

(26) Campbell, J. L. E.; Johnson, K. E. *J. Am. Chem. Soc.* **1995**, *117*, 7791.

(27) Buzzeo, M. C.; Evans, R. G.; Compton, R. G. *ChemPhysChem.* **2004**, *5*, 1106.

(28) Nöel, M. A. M.; Trulove, P. C.; Osteryoung, R. A. *Anal. Chem.* **1991**, *63*, 2892.

(29) Sahami, S.; Osteryoung, R. A. *Anal. Chem.* **1983**, *55*, 1970.

(30) Groszek, A. J.; Partyka, S.; Cot, D. *Carbon* **1991**, *29*, 821.

(31) Tarasenko, Y. A.; Lapko, V. F.; Kopyl, S. A.; Kuts, V. S.; Gerasimyuk, I. P. *Russ. J. Phys. Chem.* **2003**, *77*, 1477.

(32) Suzer, S.; Dag, O. *Can. J. Chem.* **2000**, *78*, 516.

(33) Puddephatt, R. J. In *The Chemistry of Gold*; Elsevier: Amsterdam, 1978.